Momentum distribution and valence-band reconstruction in graphite by grazing incidence $(e,2e)$ spectroscopy

S. Rioual* and S. Iacobucci†
IMAI-CNR Area Ricerca di Roma, Via Salaria km 29.300, c.p. 10, 00016 Monterotondo, Italy

D. Neri
Università degli Studi di Roma La Sapienza, Piazzale Aldo Moro, 2, 00187 Roma, Italy

A. S. Kheifets‡ and G. Stefani
Unità INFM Roma 3 and Dipartimento di Fisica, Università Roma Tre, Via Vasca Navale 84, 00146 Roma, Italy
(Received 12 May 1997; revised manuscript received 3 September 1997)

The capability of grazing angle $(e,2e)$ experiments to map momentum distribution is demonstrated. This is an application of reflection $(e,2e)$ experiments as a unique twofold spectroscopy, binding energy and momentum distribution, for solid surfaces. The reported experiments have been performed on highly oriented pyrolytic graphite at about 300-eV incident energy, grazing angle, and for ejected electron energies ranging from 3.7 to 30 eV. These experiments, interpreted in the framework of the plane-wave impulse approximation, yield the binding energy vs momentum dispersion curves of valence electron states as well as the individual π-state momentum density. Both results compare favorably with calculated graphite band structure. [S0163-1829(98)06404-2]

I. INTRODUCTION

A detailed picture of the electronic structure of solids is needed in order to obtain a fundamental understanding of their properties and to learn how to engineer new artificial materials. Ideally, one would like to measure the full spectral momentum density $\rho(\varepsilon,\mathbf{q})$ of the electronic states in solids, to obtain in the one-electron approximation both the band structure, energy ε vs momentum $\mathbf{q}$, and the momentum density of the band orbitals. The band structure of crystalline solids can be obtained with good energy resolution[1] and adequate momentum resolution by angle-resolved photoelectron spectroscopy (ARPES), but the full spectral momentum density cannot be obtained by this technique.

In recent years $(e,2e)$ spectroscopy has demonstrated the capability of measuring the spectral momentum density of crystalline and amorphous solids; both bulk and surface electronic properties can be studied by the technique.[2] The $(e,2e)$ scattering process consists of detecting, coincident in time, the scattered and ejected electrons created by an incident electron beam. The full kinematics, energy and momentum, of the electrons are measured.[3]

While $(e,2e)$ already achieves a momentum resolution comparable with ARPES, the energy resolution is significantly poorer.[4] Though the energy resolution is less than the resolution achieved in ARPES, the $(e,2e)$ technique is capable of measuring the full spectral momentum density while ARPES can measure only the band structure.

The cross section for ARPES is not proportional to the spectral momentum density for the following reasons. For energies at which ARPES is usually performed, the photon momentum is negligible; hence, the photoemission process always involves transitions between states of equal momentum. In order to define unambiguously the ejected electron momentum $\mathbf{K}_e$, the kinetic energy E_e must be large enough; as a consequence, the initial bound state must have an identically large momentum and an ''umklapp'' procedure is necessary in order to reduce the band representation to the first Brillouin zone. The umklapp relies on the energy degeneracy of states having momenta that differ by a reciprocal lattice vector $\mathbf{G}$. The same degeneracy does not hold for the amplitude of the transition matrix element, and it is impossible to unambiguously relate the photoemission cross section measured at large $\mathbf{q}$ to the initial state momentum distribution $\rho(\varepsilon,\mathbf{q})$. Furthermore, in such a high energy limit (x-ray photoemission spectroscopy) the plane-wave (PW) approximation holds; the photoemission matrix element becomes proportional to the Fourier transform (FT) of the initial state, but the phonon smearing prevents from discriminating the initial state momentum.[5] This is because in the high energy limit, reciprocal lattice vectors whose magnitude is comparable to K_e must be involved in the photoemission process. It implies[5] that the volume in momentum space, from which transitions originate and for which phonon smearing is absent, can be much smaller than the first Brillouin zone, at least at room temperature. On the contrary, at low energy the phonon smearing can be neglected but the matrix element cannot any longer be reduced to a simple FT of the initial state. This limitation on the possibility of achieving at the same time a good momentum resolution and a matrix element simply proportional to initial state FT is removed if, instead of photoemission, $(e,2e)$ experiments are used.

In the high energy limit, the plane-wave impulse approximation (PWIA) has been shown to be adequate to calculate the $(e,2e)$ cross section[6] and energy and momentum conservation can be written as

$$E_0+\varepsilon(\mathbf{q})=E_s+E_e, \tag{1}$$

$$\mathbf{K}_0+\mathbf{q}=\mathbf{K}_s+\mathbf{K}_e, \tag{2}$$

where E_0, E_s, and E_e are the incident, scattered, and ejected electron energies, respectively, and $\mathbf{K}_0$, $\mathbf{K}_s$, and $\mathbf{K}_e$ are the corresponding momenta. Within the PWIA, $\mathbf{q}$ is identified as the bound electron momentum before the collision.[7] The momentum $\mathbf{q}$ of the initial state can be varied continuously, independent of the energy of the state, throughout the different Brillouin zones by simply changing the kinematics of the collision. In $(e,2e)$ experiments the uncertainty in $\mathbf{q}$ is determined solely by experimental constraints.

The $(e,2e)$ experiments performed at high incident energy and in transmission geometry on the thin films have already shown the unique capability of this method to map the band structure and to accurately measure the associated momentum density.[2] The limitations imposed by the finite sample thickness have been recently overcome by performing the experiment in reflection geometry[8] and at grazing angle.[7] In these conditions it is possible to operate on thick samples with the enhanced surface sensitivity that is a peculiarity of the grazing incidence condition.[9] The interpretation of reflection $(e,2e)$ experiments rests on a model that assumes the inelastic ionizing collision to be assisted by an elastic mirror reflection from the surface.[10] It has been shown[11] that for incident energies of 300 eV, asymmetric kinematics, grazing angles of few degrees and ejected electron energy of few tens of eV, the experiment is feasible and a momentum selected binding-energy spectrum can be built.

The aim of the present paper is to demonstrate that the reflection geometry, as well as the transmission one, is suitable to perform both band mapping and momentum density spectroscopy.

II. EXPERIMENT

The sample, a 0001 surface of highly oriented pyrolytic graphite (HOPG), was prepared according to standard ultrahigh vacuum methods.[12] Measurements have been performed in asymmetric kinematics and under mirror reflection of the fast electron that was brought to collide with the surface at a grazing angle of 5° or 6°. Binding-energy spectra were measured by scanning E_0, typically from 300 to 340 eV, while keeping fixed E_s and E_e. The fast scattered electron was analyzed by a hemispherical deflector analyzer (HDA) tuned at 300 eV. The slow ejected electron was detected by a single pass cylindrical mirror analyzer (CMA), whose axis was parallel to the surface normal **c**. A standard coincidence electronic chain[13] was used to time correlate the two final electrons with an overall uncertainty of about 12 ns. A complete description of the coincidence spectrometer can be found elsewhere.[14]

Binding-energy spectra have been measured for six different E_e values: 3.7, 8, 14.2, 15, 21, and 30 eV. The overall energy resolution was 1.2 eV for measurements at $E_e=3.7$, 8, 14.2, 21, and 30 eV; and 3 eV for the ones at 8 (repeated with different resolution) and 15 eV. The achieved overall momentum acceptance Δq is mostly due to the CMA wide angular acceptance, while contributions from the HDA accepted solid angle, beam divergence, and energy uncertainties are negligible.

The only well-defined symmetry axis of the HOPG sample is **c**, which is perpendicular to the surface plane within 1°. The reconstructed momentum $\mathbf{q}$ [see Eq. (2)] has nonvanishing components in both directions parallel $(q_\parallel)$ and perpendicular $(q_\perp)$ with respect to **c**. Moreover, the CMA acceptance angle does not allow for azimuth resolution, while polar resolution is limited to $\pm 3°$ around 42.3° with respect to **c**. All of these experimental constraints result in averaging the measured $(e,2e)$ cross section over a roughly toroidal volume in momentum space. The projection of the torus on the basal plane is an annular area whose internal and external radii correspond to the extreme values of $|\mathbf{q}_\perp|$. Taking into account the finite analyzer angular acceptances, the spectrometer work function, and the refraction across the surface potential barrier of the sample,[15] the extreme and average values of $\mathbf{q}_\perp$ and $q_\parallel$ are reconstructed for each E_e. The values of $\mathbf{q}_\perp$ range from nearly the center up to the boundaries of the first Brillouin zone in the ΓMK plane. In the same experimental conditions, the $q_\parallel$ component ranges from the bottom to the middle of the third Brillouin zone along the ΓA direction.

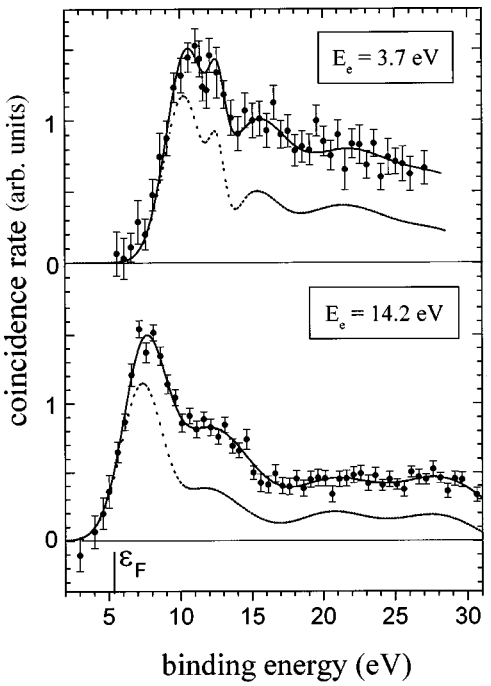

FIG. 1. $(e,2e)$ binding-energy spectra as measured on HOPG for two different ejected electron energies (E_e). The binding-energy scale origin is the spectrometer vacuum level, the Fermi level (ε_F) is also indicated. Continuous lines are best fits to the data. Dotted lines are spectra after multiple-scattering correction. (See the text for details.)

III. RESULTS AND DISCUSSION

A. Valence-band reconstruction

The $(e,2e)$ cross section, measured as a function of the binding energy, is reported in Fig. 1 for two different E_e values (3.7 and 14.2 eV). The vacuum level is the origin of the binding-energy scale, whose value has been derived from the energy conservation law. The Fermi level ε_F, as derived from an independent measurement,[15] is also indicated in the figure. The full line is a least χ^2 fit to the raw experimental

data performed by means of an analytical trial function, which is the sum of four Gaussians whose position, amplitude, and width are fitting parameters. The trial function has been adopted to mimic contributions from the four occupied bands of graphite[18] and is found to be adequate for all the measured binding-energy spectra.

The relative intensity of the features appearing in the unprocessed data is affected by multiple loss contributions that result in an ''apparent'' increase of intensity at the higher binding energies. These spurious effects are evaluated by the iterative method suggested by van Cittert.[16] The adopted deconvolution procedure is applied at the fast electron channel only, the loss probability of the slow ejected electron being about 100 times smaller.[7] The multiple loss probability for the fast electrons (incoming and scattered) has been measured, at the same glancing angle and energy resolution as the $(e,2e)$ experiment, by an angle-resolved electron energy-loss spectrum. The measured loss spectrum, once deconvoluted for the spectrometer energy resolution, yielded the loss function that has been used to remove multiple-scattering effects from the $(e,2e)$ cross section.[16] The intensity correction operated by the method is negligible only at the Fermi level, then it increases up to 60% in the vicinity of the valence-band bottom. On the contrary, the correction on the energy position of the main features is always negligible, at least within the present energy resolution. The final result of the deconvolution procedure is shown by dotted lines in Fig. 1. The multiple loss correction is found to be less important in reflection than in transmission mode experiments. These latter experiments, although performed at much higher energy, have shown a sizable coincidence count rate up to binding energies as large as the carbon K shell.[17]

The four main features appearing in the measured binding-energy spectra are ascribed to ionization events from the π, σ_3, σ_2, and σ_1 band states, from low to high binding energy, respectively. The assignment has been done on the basis of $(e,2e)$ cross section computed in PWIA and taking into account the graphite band structure.[18] It might be speculated that the kinetic energy of the ejected electron is too low for it to be considered a PW. Should that be the case, the $(e,2e)$ cross section would be determined by the joint density of states[1] (JDOS) in the volume of momentum space selected by the experimental kinematics. Though this is true in principle, in practice the experiment was performed selecting a given final state and keeping it unchanged while scanning through the initial states with different binding energies. This is similar to what happens in a constant final state photoemission experiment,[19] hence the measured cross section is dominated by initial state characters rather than by the JDOS.

By choosing different E_e values, a selection is achieved in $\mathbf{q}_\perp$ and in $q_\parallel$ (see Table I). Plotting the energy positions of the peaks appearing in the $(e,2e)$ spectra vs the correspondent average values of $\mathbf{q}_\perp$, a mapping of the HOPG band dispersion is obtained. This is shown in Fig. 2, where the experimental result is compared with the calculated band structure for a graphite single crystal.[18] Because of the aforementioned averaging on $\mathbf{q}_\perp$, the experiment does not discriminate among different directions in the ΓMK plane, while the calculation does. From Fig. 2 it is evident that a sharp difference does not exist between bands calculated along ΓM and ΓK directions. Hence, it is reasonable to compare the results with the dispersion calculated along both these high symmetry directions. Despite the poor momentum resolution, a good agreement is evident for the outermost bands over the entire measured momentum range, especially for what concerns the π band. Some disagreement for the peaks assigned to the σ_1 and σ_2 bands is found. In particular, the σ_1 experimental location is deeper than theoretically expected by about 1.5 eV. A similar discrepancy, even though smaller, is found in the dispersion curve measured in a transmission $(e,2e)$ experiment.[20] Intrinsic loss contributions cannot be excluded as the origin of these features.[21]

TABLE I. Electron momentum values reconstructed in reflection $(e,2e)$ experiments for the π band of HOPG. The module of the momentum at the center of the volume sampled by the experiment (q) is reported for each ejected electron energy (E_e) in the last column. The extreme values of the $\mathbf{q}$ components along the directions perpendicular $(q_\perp)$ and parallel $(q_\parallel)$ to $\mathbf{c}$, as determined by the experimental acceptances, are also reported.

E_e (eV)	$q_\perp^{\min}$ (au)	$q_\perp^{\max}$ (au)	$q_\parallel^{\min}$ (au)	$q_\parallel^{\max}$ (au)	q (au)
3.7	0.35	0.57	0.68	0.7	0.82
8	0.35	0.67	0.83	0.86	0.985
14.2	0.47	0.91	0.95	1	1.194
21	0.59	1.19	1.1	1.17	1.411
30	0.65	1.35	1.2	1.29	1.596

B. Momentum distribution

The measured binding-energy spectra have been interpreted in the framework of the PWIA. Within this scheme the amplitude of the fivefold differential cross section is proportional, through a kinematical factor $F(\mathbf{K}_s,\mathbf{K}_e)$, to the momentum density $\rho(\mathbf{q})$:[2]

$$\frac{d^5\sigma}{d\Omega_e d\Omega_s dE} = F(\mathbf{K}_s,\mathbf{K}_e)\rho(\mathbf{q}).$$

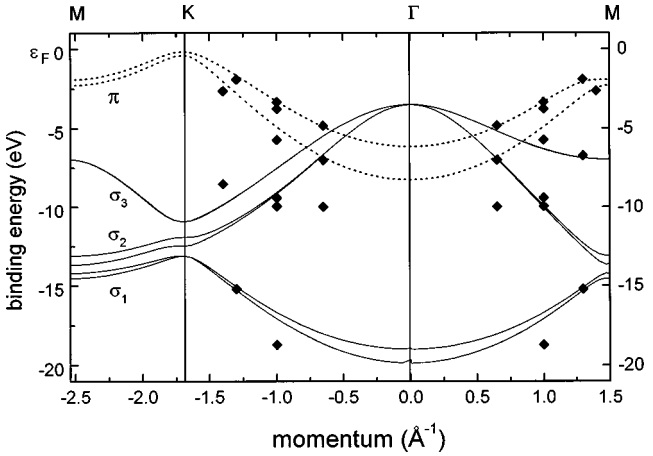

FIG. 2. Comparison between HOPG valence bands reconstructed by reflection $(e,2e)$ spectra and theoretical valence-band structure. Diamonds correspond to peak locations in $(e,2e)$ binding-energy spectra, continuous lines are taken from the calculation of Ref. 18 for a graphite single crystal.

The measured cross sections have been brought on the same relative scale by normalizing the intensities to an identical incident current.

Let us focus the attention on the cross-section amplitude corresponding to the π band. The reason for concentrating on this transition alone rests on two facts: (i) the statistical uncertainty is minimal for this transition at all ejected energies; (ii) being the last occupied state, its intensity will not be contaminated by multiple scattering effects, no matter how good the deconvolution procedure is.

The experiment measures a quantity that is directly proportional to the integrated cross section:

$$\sum = \int_{\Delta \mathbf{q}} \frac{d^5\sigma}{d\Omega_e d\Omega_s dE} d^3q.$$

Assuming the kinematical factor F to be constant within the volume of the momentum space sampled by the experiment ($\Delta \mathbf{q}$), the π-band peak amplitude is

$$I_\pi = CF\Delta E \int_{\Delta \mathbf{q}} \rho_\pi(\mathbf{q}) d^3q,$$

where C is a suitable normalization constant and ΔE is the overall coincidence energy resolution.[13] The quantity $I_\pi / F\Delta E$ was measured for several ejected electron energies and is plotted in Fig. 3 vs the average momentum q whose components of $q_\parallel$ and $q_\perp$ are given in Table I. In the same figure is plotted the theoretical π-band momentum density integrated over the range of the experimental $\Delta \mathbf{q}$:

$$\int_{\Delta \mathbf{q}} \rho_\pi(\mathbf{q}) d^3q = \int_{q_{\parallel}\min}^{q_{\parallel}\max} dq_\parallel \int_{q_{\perp}\min}^{q_{\perp}\max} dq_\perp \int_0^{\pi/6} d\theta_q \rho_\pi(\mathbf{q}).$$

Here the integration over the azimuthal angle θ_q simulates the rotational disorder of the HOPG sample. The limits of integration over $q_\parallel$ and $q_\perp$ are given in Table I for each ejected electron energy. The π-band momentum density $\rho_\pi(\mathbf{q})$ was calculated using the method described in Ref. 18.

The theoretical integrated momentum density (open squares) has been normalized to the maximum of the experimental distribution (solid circles). The agreement between theory and experiment is good, except for the point at the lowest momentum value, which corresponds to the lowest ejected electron energy. This is not surprising, because the PWIA is certainly a crude approximation for 3.7-eV electrons.

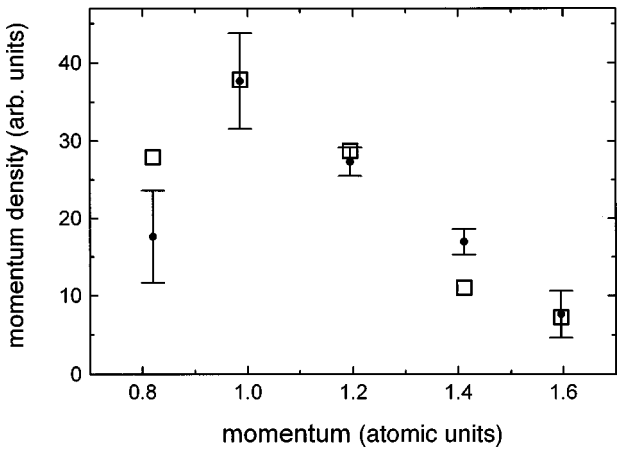

FIG. 3. Measured and theoretical momentum distribution for π-band electrons in graphite (arbitrary units). Solid circles are experimental determinations by $(e,2e)$ performed in reflection mode on HOPG surface. Open squares indicate the theoretical momentum density (Ref. 18) integrated over the volume of the momentum space sampled by the experiment. The two distributions are normalized to the same maximum value for comparison.

In conclusion, the present paper demonstrates that the grazing angle $(e,2e)$ reflection experiments yield a twofold spectroscopy, binding energy and momentum density, for surfaces of thick crystals. The main assumption upon which the data analysis is based is the PWIA. After a suitable subtraction of the multiple-scattering effects, the dispersion curves of the HOPG valence states have been measured and found to be in good agreement with the calculated ones. A fair agreement between the experimental and the calculated momentum density of the π band is also found. These findings are evidence for the capability of the technique to measure momentum distributions of selected bands and for adequacy of the reaction model assumed.

ACKNOWLEDGMENTS

This work has been made possible by the financial support of EEC Human Capital and Mobility, Contract No. ERBCHRXCT930359, and Progetto Finalizzato Chimica Fine del CNR.

*Present address: Lab. Coll. Electr. at Atom., Université de Bretagne Occidentale, Brest, France.

†Author to whom correspondence should be addressed.

‡Permanent address: RSPhysSE, Australian National University, Canberra, ACT 2601, Australia.

[1] H. Lüth, *Surfaces and Interfaces in Solids* (Springer-Verlag, Heidelberg, 1993).

[2] M. Vos and I. E. McCarthy, Rev. Mod. Phys. **67**, 713 (1995).

[3] G. Stefani, L. Avaldi, and R. Camilloni, J. Phys. IV, Colloq. C **6/3**, 1 (1993).

[4] S. A. Canney, M. J. Brunger, I. E. McCarthy, P. J. Storer, S. Utteridge, M. Vos, and E. Weigold, J. Electron Spectrosc. Relat. Phenom. **83**, 65 (1997).

[5] C. S. Fadley, in *Electron Spectroscopy Principles and Techniques*, edited by C. R. Brundel and A. D. Baker (Academic, New York, 1978), p. 140.

[6] I. E. McCarthy and E. Weigold, Rep. Prog. Phys. **54**, 789 (1991).

[7] S. Iacobucci, L. Marassi, R. Camilloni, S. Nannarone, and G. Stefani, Phys. Rev. B **51**, 10 252 (1995).

[8] J. Kirschner, O. M. Artamov, and A. N. Terekhov, Phys. Rev. Lett. **69**, 1711 (1992).

[9] S. Iacobucci, P. Letardi, M. Montagnoli, P. Nataletti, and G. Stefani, J. Electron Spectrosc. Relat. Phenom. **67**, 479 (1994).

[10] D. L. Mills, Surf. Sci. **48**, 59 (1975).

[11] S. Iacobucci, L. Marassi, R. Camilloni, B. Marzilli, S. Nannarone, and G. Stefani, J. Electron Spectrosc. Relat. Phenom. **76**, 109 (1995).

[12] R. G. Musket, W. McLean, C. A. Colmenares, D. Makowiecki,

and W. J. Siekhaus, Appl. Surf. Sci. **10**, 143 (1982).
[13] G. Stefani, L. Avaldi, and R. Camilloni, in *New Directions in: Research with Third Generation Soft X-ray Synchrotron Radiation Sources*, Vol. 254 of *NATO Advanced Study Institute, Series E: Applied Sciences*, edited by A. F. Schlachter and F. J. Wuilleumier (Kluwer Academic, Dordrecht, 1994), pp. 161–190 and references therein.
[14] R. Camilloni, S. Iacobucci, L. Marassi, S. Nannarone, and G. Stefani, I1 Vuoto XXIV, **64** (1995).
[15] A. Ruocco (private communication).
[16] P. H. van Cittert, Z. Phys. **69**, 298 (1931).
[17] M. Vos, P. Storer, A. S. Kheifets, I. E. McCarthy, and E. Weigold, J. Electron Spectrosc. Relat. Phenom. **76**, 103 (1995).
[18] A. Kheifets and M. Vos, J. Phys.: Condens. Matter **7**, 3895 (1995).
[19] A. R. Law, M. T. Johnson, H. P. Hughes, and H. A. Padmore, J. Phys. C **18**, L297 (1985).
[20] M. Vos, P. Storer, S. A. Canney, A. S. Kheifets, I. E. McCarthy, and E. Weigold, Phys. Rev. B **50**, 5635 (1994).
[21] N. A. Krasil'Nikova and N. M. Persiantseva, Phys. Lett. **69A**, 287 (1978).